Int J Adv Manuf Technol (2014) 71:1801–1810
DOI 10.1007/s00170-014-5608-y

ORIGINAL ARTICLE

Optimal CNC plunge cutter selection and tool path generation for multi-axis roughing free-form surface impeller channel

F. Y. Han · D. H. Zhang · M. Luo · B. H. Wu

Received: 14 June 2013 / Accepted: 7 January 2014 / Published online: 24 January 2014

Abstract Plunge milling is the most effective way for rough machining of impeller parts, but previous research had not considered the optimization of plunge cutter selection and tool path. In this paper, a new method for optimizing the plunge cutter selection and tool path generation in multi-axis plunge milling of free-form surface impeller channel is proposed in order to improve the efficiency in rough machining. Firstly, in the case of fixing a rotation axis at a certain angle in five-axis machine, a mathematical representation is formulated for the geometric model of the cutter interfering the impeller, and an optimization model of the cutter size is established at a cutter contact point on the impeller channel surface, so the largest tool could be determined. Secondly, by analyzing the machine tool movement characteristics, the geometric constraint model of the plunge tool path which relative to the largest tool, step distance, and row space is established, and a tool orientation calculation method of impeller channel machining is given, and then, the plunge tool path and tool orientation could be obtained. Finally, the generated tool path and tool orientation are simulated and verified in practical processing. Simulation and experimental result shows that the rough machining efficiency of the impeller part is improved up to 40 % with this method.

Keywords Impeller channel · Plunge milling · Tool path · Tool orientation · The largest tool

1 Introduction

Plunge milling is the most effective way for rough machining, as it can rapidly mill away a large volume of metal in the machining process, and it is suitable for machining some complex surface parts, such as free-form surface impeller. Although the plunge milling as a new processing technology is widely used in industry, the research of it is still very insufficient.

In only few published literatures, El-Midany et al. [1] presented a novel method called "Ocfill" for optimizing the selection of multi-plungers sizes and tool path. The Ocfill method was used to fill a 2D area with a number of overlapped circles with multi-diameters. The 2D area was expressed as a plunged area, and the circles were known as the plunged holes. Although Ocfill method enhanced the filling of plunged area, the direction of inclination angle of the filling was always selected to be constant and parallel to zero direction. Tawfik [2] proposed a novel algorithm to calculate the optimal inclination angle of filling and to fill the plunged area with multi-plungers sizes. This algorithm used the geometry of the 2D area of the shape that is being cut to estimate the optimal inclination angle of filling. It was found that the optimal inclination angle for filling of the plunged area was the same direction as the longer width of the equivalent convex polygon of the boundary contour, and the residual volume was minimized when comparing the proposed algorithm with the previous method [1]. Wakaoka et al. [3] studied the high-speed and high-accuracy plunge cutting for vertical walls. Gan et al. [4] presented a novel method of tool path planning for plunge milling of pocket walls based on constant scallop height. The results indicated that iso-scallop machining achieved the specified machining accuracy with fewer cutter location (CL) points than existing tool path generation approaches. Liang and Wang [5] presented a method for plunge milling, a ruled surface impeller, which improved the efficiency of rough machining of impeller parts and made up the deficiency of commercial computer-aided manufacturing (CAM) software in five-axis plunge milling, but the calculation of row space and step distance based on the boundary tool orientations made the method to have limitations in application.

F. Y. Han · D. H. Zhang · M. Luo · B. H. Wu (✉)
Key Laboratory of Contemporary Design and Integrated Manufacturing Technology (Northwestern Polytechnical University), Ministry of Education, Xi'an 710072, China
e-mail: Baohai_WU@163.com

Meanwhile, the five-axis tool path planning method for plunge milling has also been studied by Hu et al. [6], and the tool path for plunge milling blisk's tunnel region was generated by linking the corresponding points between CL points and tool axis drive curves in this method, but it did not consider row space and step distance calculation criteria, so the plunge milling material removal rate and efficiency cannot be guaranteed. In order to reduce processing costs of blisk, the four-axis tool path planning method for plunge milling has also been studied [7]. In this method, first, the ruled envelope surface was directly created from the surface of the blade, and then, the ruled envelope surface was offset; the errors were inevitable when calculating the tool path according to the offsetting ruled envelope surface, since the offsetting surface was still regarded as a ruled envelope surface. Ren et al. [8] improved the above method [10]; first, the surface of the blade was directly offset, the offsetting blade surface was generated, and then, the ruled envelope surface was created from the offsetting blade surface, so the errors can be fundamentally avoided when calculating the tool path according to the ruled envelope surface. Nevertheless, the disadvantages of this approach were that the tool paths have not been optimized, and the collision problems between the plunge cutter and the blades have not been solved.

Selection of a plunge cutter is important for plunge milling, since a larger plunge cutter size helps to obtain efficient plunge tool path which is closely related to the row space and the step distance, whereas the row space and the step distance are both determined by the cutter size. In the actual processing, a human process planner selects the smaller tool size using his/her prior experience or from handbooks based on the part geometry and technological requirements. Disadvantages of this manual approaches led to the development of automated approaches that aimed to reduce the processing time. The correct choice of cutting tool is determined by the overall part configuration, rather than by individual contour section or workpieces. Therefore, some papers have been written for solving plunge cutter selection problem in recent years but mainly aimed at the cutter selection of cavity type parts [9–19], Nadjakova and McMains [9] described an approach to finding the radii of an optimal set of cutters for machining a pocket by using Voronoi diagrams. Based on their Voronoi diagrams, Elber et al. [10] provided a scheme to generate trochoidal tool paths for high-speed machining of free-form pockets. Besides the Voronoi diagram-based methods, Chen and Zhang [11] plotted the radius graph of the maximum circles along the medial axis of a pocket in order to find the largest tool for finish cutting of a free-form pocket without gouging and interference. Moreover, Chen and Liu [12] proposed a new intelligent approach to select multiple largest cutters for aggressive roughing of sculptured surface in three-axis machine. Yang et al. [13] decomposed pockets into regular features to best fit multiple cutters of various sizes so that they can efficiently cut the corresponding features without overcut, and then Joneja et al. [14] applied this greedy technique to different layers of pockets surrounded by sculptured surfaces. Yao et al. [15, 16] proposed a geometric algorithm to determine the largest feasible cutter size for 2D milling operations, and an optimal sequence of cutters for machining a set of two-and-a-half-dimensional parts was selected automatically. Zhang and Li [17] tried to select multiple tools to achieve the optimal roughing of pockets with an arbitrary shape in terms of the minimum machining time and the maximum material removal rate. Narayanaswami and Choi [18] provided a grid-based 3D navigation algorithm for generating CNC tool paths for three-axis milling of pockets with sculptured concave surfaces. D'Souza et al. [19] introduced an efficient method of finding the tool sequence with the minimum cost of rough machining of free-form pockets on a three-axis milling machine. Unfortunately, no research has been found that optimizes the cutter selection for multi-axis milling of complex impeller parts.

To address the above problems, an automated approach to calculate the largest cutter size and tool paths for five-axis rough milling of free-form surface impeller with high efficiency is studied. This paper includes four sections. In Section 2, a mathematical representation for the geometric model of the cutter gouging the impeller is formulated, and an optimization model of the largest cutter is established in the case of fixing the swing spindle at a certain angle in five-axis machine. In Section 3, a geometric constraint model of tool path is established to obtain the plunge tool path by analyzing the machine tool movement characteristics. Then, in Section 4, a practical example is provided to demonstrate the validity of this approach. Finally, conclusions are given in Section 5.

2 The largest cutter size calculation for impeller channel machining

On a five-axis machine tool with swing spindle, if the angle of swing spindle is fixed at an appropriate angle, it can increase the rigidity of five-axis machine tool and significantly improve the cutting stability, especially beneficial for plunge milling. Because the movement of plunge milling is performed in a fixed axial direction which remains unchanged in the movement process when machining a single point. Thus, supposing the swing spindle is fixed at an angle of 45°, an approach to calculate the largest cutter for milling the impeller channel is proposed under this mechanical structure (see Fig. 1), and the details are introduced in this section.

$$\begin{cases} X_W = Z_M \\ Y_W = X_M \\ Z_W = Y_M \end{cases}$$

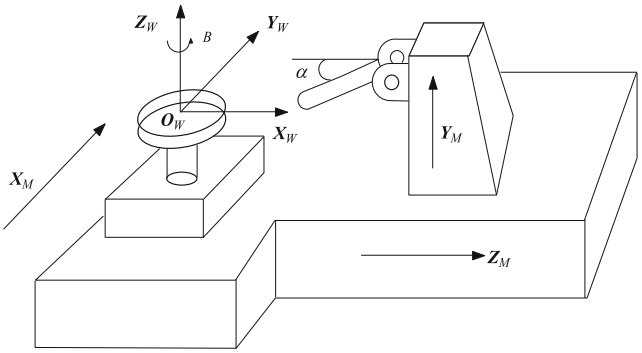

Fig. 1 Five-axis machine tool

2.1 Feasible tool orientation representation in the workpiece coordinate system

In this section, the feasible tool orientation in the workpiece system is calculated first; namely, a visibility map [20–22] of a parametric surface represents the feasible tool direction along which a cutter that can safely reach the surface is determined first.

As shown in Fig. 1, assume that the workpiece coordinate system $\{O_W; X_W, Y_W, Z_W\}$ and the machine coordinate system $\{O_M; X_M, Y_M, Z_M\}$ are met the right-hand rule and their coordinate origins are coincided with each other (see Fig. 1), so there has the following relationship.

A five-axis machine tool has three translations and two rotation axes (see Fig. 1). It can move linearly along the X_M- Y_M- and Z_M-axis in the machine coordinate system, and simultaneously, the pallet on the work table can rotate around its axis, which is called *B*-axis, and the swing spindle can rotate around its axis, which is called *A*-axis. The rotation angle of *B*-axis is denoted by β, and its range is [0,360°]; the rotation angle of *A*-axis is considered as a constant value α, because *A*-axis is assumed to be a fixed axis in this study. In this case, the five-axis machine tool (see Fig. 1) is equivalent to a four-axis machine tool, but it is unlike a conventional four-axis machine tool. During the tool path planning, when the work table rotates around its axis with angle β, the impeller workpiece rotates around the Z_W-axis in the workpiece coordinate system at the same time; thus, the relative orientation between the tool axis and the impeller is changed. The rotation of the work table is considered to be the tool axis's rotation around the Z_W-axis, so the tool axis is no longer bounded in the tool motion plane of the conventional four-axis machining, but it is constrained on a cone surface that its rotation axis is Z_W-axis and its half-apex angle is $\pi/2-\alpha$. So the tool axis which meets the constraint condition of the five-axis machine (see Fig. 1) is located on a series of cone surfaces, and the rotation axis of these cones is parallel to Z_W-axis, and the half-apex angle of these cones is $\pi/2-\alpha$.

As shown in Fig. 1, in the workpiece coordinate system $\{O_W; X_W, Y_W, Z_W\}$, assume that the rotation axis of Z_W-axis is (0,0,1), when the tool is rotating around Y_W-axis with angle α in clockwise, the initial tool axis can be expressed as

$$T_{W0} = \begin{bmatrix} \sin\alpha \\ 0 \\ \cos\alpha \end{bmatrix}. \quad (1)$$

Then, when the work table rotates around the Z_W-axis with an angle β, that is equal to the tool axis rotating with an angle $-\beta$ on a cone surface which passes through the work table center and its half-apex angle is $\pi/2-\alpha$. According to the rotation transformation method of computer graphics, when the work table rotates, the representation of tool orientation $T_W(\beta)$ in the workpiece coordinate system is

$$T_W(\beta) = \begin{bmatrix} \cos\alpha \cdot \cos(-\beta) \\ \cos\alpha \cdot \sin(-\beta) \\ \sin\alpha \end{bmatrix} \quad (2)$$

where $T_W(\beta)$ represents the tool orientation when the work table rotates around the Z_W -axis with an angle β in the workpiece coordinate system.

2.2 Rotation angle range of interference-free tool axis

The feasible tool orientation is considered to be constrained on a cone surface with a half-apex angle $\pi/2-\alpha$ in the five-axis machining (see Fig. 1). The rotation axis of the cone is Z_W-axis, and the feasible tool orientation can rotate around the Z_W-axis with angle β on the cone surface, so the tool orientation can be represented with rotation angle β of the Z_W-axis.

Due to the complex blade shape of an impeller and small tool accessible space between two adjacent blades, the selected cutter cannot safely access each impeller channel point in all of the feasible tool orientations. For machining the impeller channel surface, the cutter has to access every impeller channel point along a feasible tool orientation without gouging or colliding with the surrounding blades. This kind of tool orientation is called valid tool orientation, and all valid tool orientations of an impeller channel point can be represented with a range of angle β. Hence, it is necessary to find out the range of angle β of each impeller channel point for a given cutter, which is addressed in this section.

In the workpiece coordinate system, suppose S is the machined surface of an impeller channel, and $C(u,v)$ is a cutter contact (CC) point on the surface S, $T_W(\beta)$ is a valid tool orientation when milling this CC point with a multi-axis machine tool (see Fig. 1), and $n(u,v)$ is the surface normal vector of this CC point. As shown in Fig. 2, $T_W(\beta)$, $n(u,v)$, and

unit vector $\boldsymbol{v}$ are located in the same plane, and those three vectors form a right triangle, both unit vectors of $T_W(\beta)$ and $\boldsymbol{v}$, are normal to each other. Based on the valid tool orientation $T_W(\beta)$ and the unit surface normal $n(u, v)$, the unit vector $\boldsymbol{v}$ can be found as

$$v = \begin{bmatrix} v_x \\ v_y \\ v_z \end{bmatrix} = \begin{bmatrix} \dfrac{n_x - \left(T_{W,x}(\beta)\cdot n_x + T_{W,y}(\beta)\cdot n_y + T_{W,z}(\beta)\cdot n_z\right)\cdot T_{W,x}(\beta)}{\sqrt{\left(n_x\cdot T_{W,y}(\beta) - n_y\cdot T_{W,x}(\beta)\right)^2 + \left(n_y\cdot T_{W,z}(\beta) - n_z\cdot T_{W,y}(\beta)\right)^2 + \left(n_z\cdot T_{W,x}(\beta) - n_x\cdot T_{W,z}(\beta)\right)^2}} \\ \dfrac{n_y - \left(T_{W,x}(\beta)\cdot n_x + T_{W,y}(\beta)\cdot n_y + T_{W,z}(\beta)\cdot n_z\right)\cdot T_{W,y}(\beta)}{\sqrt{\left(n_x\cdot T_{W,y}(\beta) - n_y\cdot T_{W,x}(\beta)\right)^2 + \left(n_y\cdot T_{W,z}(\beta) - n_z\cdot T_{W,y}(\beta)\right)^2 + \left(n_z\cdot T_{W,x}(\beta) - n_x\cdot T_{W,z}(\beta)\right)^2}} \\ \dfrac{n_z - \left(T_{W,x}(\beta)\cdot n_x + T_{W,y}(\beta)\cdot n_y + T_{W,z}(\beta)\cdot n_z\right)\cdot T_{W,z}(\beta)}{\sqrt{\left(n_x\cdot T_{W,y}(\beta) - n_y\cdot T_{W,x}(\beta)\right)^2 + \left(n_y\cdot T_{W,z}(\beta) - n_z\cdot T_{W,y}(\beta)\right)^2 + \left(n_z\cdot T_{W,x}(\beta) - n_x\cdot T_{W,z}(\beta)\right)^2}} \end{bmatrix}. \tag{3}$$

Then, the equation of the CL point P is derived as

$$P(u,v,\beta) = \begin{bmatrix} P_x(u,v,\beta) \\ P_y(u,v,\beta) \\ P_z(u,v,\beta) \end{bmatrix} = \begin{bmatrix} C_x(u,v) + R\cdot v_x \\ C_y(u,v) + R\cdot v_y \\ C_z(u,v) + R\cdot v_z \end{bmatrix}.$$

Suppose $Q(u_i, v_i)$ (i=1,2,…,n) is the checking points of an impeller blade surface, $P(u_0, v_0, \beta)$ is a CL point. The perpendicular point on the tool axis can be found, whose parameter l_i is

$$l_i = \begin{cases} (Q_x(u_i,v_i) - P_x(u_0,v_0,\beta))\cdot T_{W,x}(\beta) + \\ \left(Q_y(u_i,v_i) - P_y(u_0,v_0,\beta)\right)\cdot T_{W,y}(\beta) + \\ (Q_z(u_i,v_i) - P_z(u_0,v_0,\beta))\cdot T_{W,z}(\beta). \end{cases}$$

The distance between the checking point on the blade surface and the tool axis can be calculated as follows:

$$d_i = \begin{bmatrix} \left(Q_x(u_i,v_i) - l_i\cdot T_{W,x}(\beta) - P_x(u_0,v_0,\beta)\right)^2 + \\ \left(Q_y(u_i,v_i) - l_i\cdot T_{W,y}(\beta) - P_y(u_0,v_0,\beta)\right)^2 + \\ \left(Q_z(u_i,v_i) - l_i\cdot T_{W,z}(\beta) - P_z(u_0,v_0,\beta)\right)^2 \end{bmatrix}^{\frac{1}{2}}. \tag{4}$$

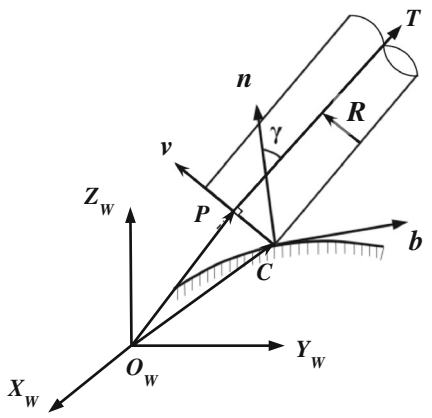

Fig. 2 Workpiece coordinate system

Since the distance between the checking point and the tool axis vector of the cutter location point can be obtained by Eq. (4), then the interference-free rotation angle can be obtained from the method based on distance monitoring. If the distance between any tool axis which corresponds to a rotation angle and each checking point meets the following condition (Eq. (5)), there is no interference occurred. The non-gouging and non-interference conditions are listed in the following:

$$\begin{cases} d_i \geq 0, l_i < 0 \\ d_i \geq R, 0 \leq l_i \leq l_T \\ d_i \geq R, l_T < l_i \end{cases} \tag{5}$$

where R represents the cutter radius, and l_T is the cutter length.

If at an impeller channel CC point Eq. (5) cannot be satisfied, it means that the cutter will overcut the impeller part in machining. By using the mathematical representation, whether the selected cutter gouges or collides with the impeller can be found quickly, if the answer is yes, the tool orientation of the angle β is invalid; otherwise, the angle β is valid.

For a given cutter, there are three steps to calculate the valid angle β during machining. Firstly, the rotation angle β corresponding to the initial tool axis $T_{W0}(\sin\alpha, 0, \cos\alpha)$ is considered as 0°, and Eq. (5) is used to judge whether there has interference under the initial tool axis. Secondly, if there has no interference, the angle β is increased to a larger one until it does not meet Eq. (5). Finally, the maximum and minimum value of the valid angle β without interference was written down. Since the range of angle β is [0,360°], so the valid angle β without interference is also within the range [0,360°], which is represented as [$\beta_{\min}$, $\beta_{\max}$].

2.3 The largest cutter size calculation

The valid tool orientation of each CC point corresponds to a range of angle β, the range of angle β is different at different

CC points, and it should be determined in order to find the largest cutter to mill the impeller channel surface.

2.3.1 Relationship between cutter size and range of valid angle β

Suppose a cutter of radius R is used to mill the impeller channel surface, a CC point on the impeller channel surface $C(u_i, v_i)$ (i=1,2,…,m_{CC}) is to be cut, the impeller workpiece must rotate around the rotation axis Z_W−axis with angle β_i so that the cutter can touch the impeller channel at this point without collision. If the cutter can safely access the CC point along a tool orientation of angle β, this angle is valid. In general, there is a range of β_i [$\beta_{i,\min}$,$\beta_{i,\max}$], each of which represents a valid tool orientation. Thus, this range is called the valid range of β_i for the impeller channel CC point. On the contrary, it is easy to understand that by increasing the cutter radius R, the valid β_i range will be reduced. Until the cutter radius reaches maximum, the β_i range is minimum with only one valid tool orientation of a single value of β_i. This means that, in this critical situation, any larger cutter cannot safely access the impeller channel CC point. In other words, if the cutter cannot access the impeller channel point in any feasible tool orientation, the range of angle β_i is void. Therefore, the cutter size directly affects the range of valid angle β_i. To represent the above relationship in this work, the valid β_i range [$\beta_{i,\min}$, $\beta_{i,\max}$] is a function of the radius of the cutter that can cut this impeller channel CC point $C(u_i, v_i)$, denoted as $R_{i,\alpha}$. This function is represented as

$$\left[B_{i,\min}, B_{i,\max}\right] = f\left[C(u_i, v_i), R_{i,\alpha}, B_i\right] \tag{6}$$

where $\beta_i \in [0,360°]$ and α is fixed at 45° in this study.

2.3.2 Algorithm procedure

In general, if the root of the surrounding blades of an impeller channel can be machined without interference by a given cutter, then the whole impeller also can be machined without interference by this cutter. Since the root of surrounding blades of an impeller channel is the most difficult part to be machined, usually, the given cutter is said to be the available machining cutter. According to the analysis of Section 2.3.1, there exists the available largest machining cutter in milling, given an impeller part. The brute force approach is conducted in this section in order to find out the largest cutter.

Suppose the CC point of cleanup tool path of the impeller channel on one side is $C=\{C_1(u_1,v_1), C_2(u_2,v_2), \ldots, C_k(u_k, v_k)\}$, and the cleanup tool path is varied as the increase of the cutter radius. The brute force approach for this issue follows the general procedures:

Step 1 Suppose the angle of swing spindle is fixed at an appropriate angle α ($0°<\alpha<90°$), and there are some available cutters in standard size, such as $[R_1, R_2, \ldots, R_i \ldots, R_{m_T}]$, where m_T represents the number of the available cutters, and the largest cutter should be selected from this list.

Step 2 According to Section 2.2, the valid angle range which corresponds to the feasible tool orientations of every CC point on the cleanup tool path is calculated when using the initial cutter R_1 as the machining cutter, and the valid angle range can be represented as $\left\{w_{R_1,1}, w_{R_1,2}, \ldots, w_{R_1,k}\right\}$, where k represents the number of the CC point on the cleanup tool path, and R_1 indicates the cutter radius. The intersection of all the valid angle ranges can be expressed as $\Omega_{R_1} = \left\{w_{R_1,1} \cap w_{R_1,2} \cap, \ldots, \cap w_{R_1,k}\right\}$.

Step 3 If the intersection of Ω_{R_1} is not void, increase the cutter radius to R_2 and repeat the step 2, and so on, and according to the cutter radius list $[R_1, R_2, \ldots, R_i \ldots, R_{m_T}]$, calculate the intersection Ω_{R_i} of all the valid angle ranges at each CC point until the intersection Ω_{R_i} is void, where $i \in [1, m_T]$. There are two possible situations when the intersection Ω_{R_i} is void: one case is that every element within the intersection Ω_{R_i} is not void, but there is no intersection, and another case is that any element within the intersection Ω_{R_i} is void and results in a void intersection. On the first situation, it means that the largest cutter size is R_i, and on the second situation, the largest cutter size is considered to be R_{i-1}. Then, write down the largest cutter size as $R_{\text{largest},1}$, so $R_{\text{largest},1}$ is the largest cutter for the cleanup machining of one side of the impeller channel.

Step 4 In terms of the above steps, the largest cutter size $R_{\text{largest},2}$ for the cleanup machining of another side of the impeller channel is obtained, and then, the largest cutter size for the whole impeller machining can be calculated as

$$R_{\text{largest}} = \min\left(R_{\text{largest},1}, R_{\text{largest},2}\right) \tag{7}$$

3 Tool path calculation of plunge milling

Plunge milling is an efficient method for rough machining. In plunge milling, small step distance and row space may result in dense cutting line which will cost much processing time. Therefore, too many cutting lines will make the plunge milling lose its high production efficiency, although it can get a better surface quality. On the contrary, large step distance and row space may result in sparse cutting line which will bring much residues metal in milling. Hence, too little cutting lines will make the plunge milling lose its machining precision, although it can get a high production efficiency. Accordingly, the value of step distance and row space should meet the

requirement of machining precision and high production efficiency simultaneously. So the determination of step distance and row space should be considered from two aspects. In this section, an approach is presented to determinate the step distance and the row space considering the above factors.

3.1 Tool path calculation

In general, the radial cutting depth α_e is defined as the row space, and s represents the step distance along the side direction in plunge milling, as shown in Fig. 3. The maximum radial cutting depth $\alpha_{e,\max}$ depends on the blade size of the plunger d_f [23], and the maximum radial cutting depth is expressed as

$$\alpha_{e,\max} = d_f \cdot \cos k_r \tag{8}$$

where k_r is tool cutting edge angle, but the blade size d_f mainly determines by the diameter of plunger. According to the approach discussed in Section 2.3, the largest cutter size can be determined, and then, the maximum row space can be obtained by solving Eq. (8).

As we have known, there is a constraint relationship among cutter size, step distance, and row space in numerically controlled (NC) machining, which make the plunge tool path meet the requirements of machining precision and efficiency at the same time. Once the cutter size and the row space are determined, the constraint relationship among cutter size, step distance, and row space can be established in the following text.

Firstly, a series of circular curves with the same radius of gyration in the impeller channel surface are determined in the machine coordinate system; these circular curves are denoted as $\{S_1,S_2,\ldots,S_i,S_{i+1},\ldots,S_n\}$, and the distance of two adjacent curves in the height direction of the impeller is the radial cutting depth α_e. Assume that the initial CL path is distributed in these circular curves $\{S_1,S_2,\ldots,S_i,S_{i+1},\ldots,S_n\}$, S_i and S_{i+1} are two adjacent circular curves on the impeller channel surface, and the distance of them is α_e, as shown in Fig. 4.

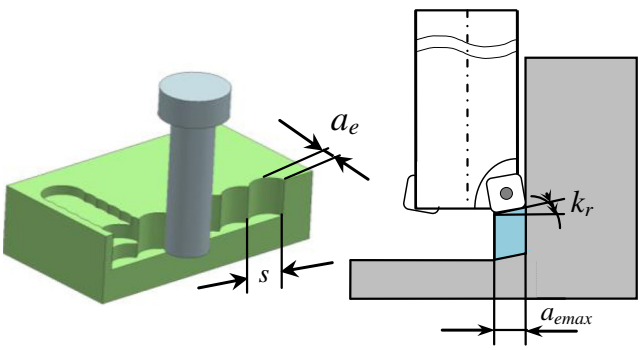

Fig. 3 Plunge milling schematic

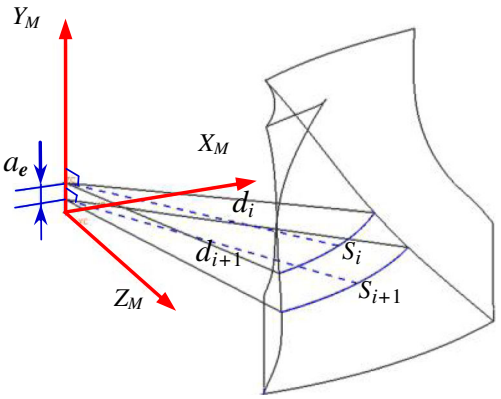

Fig. 4 Revolution surfaces of impeller channel

Secondly, the initial CL path S_i is projected to the plane $X_M O_M Y_M$ in the machine coordinate system along the direction which is vertical to the plane $X_M O_M Y_M$ (the direction of Z_M-axis) in order to make the x-and y-coordinate values remain unchanged after projection. S_i' is the projection curve on the plane $X_M O_M Y_M$ as shown in Fig. 5. In the machine coordinate system, the bottom of the tool section surface which is perpendicular to the tool movement direction is a circular surface before projecting, and its projection surface on the plane $X_M O_M Y_M$ is an ellipse surface (see Fig. 5). O_i' and O_{i+1}' are two adjacent points on the plane $X_M O_M Y_M$, and there are two projection points of the CL points O_i and O_{i+1} on the initial tool path S_i; M and N are two intersection points of the two adjacent ellipse surfaces which are the projection surface of the tool section surface, and point P is the intersection point of line $O_i'O_{i+1}'$ and lines M and N.

Finally, assume that the coordinate value of the point O_i' is (x_i, y_i) (it can be obtained from the corresponding point O_i (X_i, Y_i), since the X- and Y-coordinate value remains unchanged after projection). Based on the requirement of high efficiency and precision, the constraint model is established to obtain the next point $O_{i+1}'(x_{i+1},y_{i+1})$, the expression of the constraint model is as follows:

$$\begin{cases} l_m = \min(MP, PN) \\ l_m \geq a_{e_{\max}}/2. \end{cases} \tag{9}$$

The coordinate value of projection point O_{i+1}' is obtained by solving Eq. (9) with the penalty function, and then, the X-

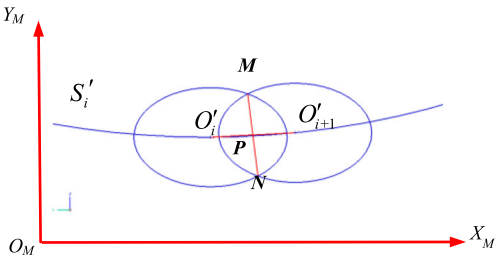

Fig. 5 Tool center trajectory projection

and *Y*-coordinate value of the point O_{i+1} can be obtained in the machine coordinate system $\{O_M; X_M, Y_M, Z_M\}$, and it is represented as

$$X_{i+1} = x_{i+1}, Y_{i+1} = y_{i+1}.$$

Since the different CL points on the same initial tool path have the same value of *Z*-axis and the distance of two adjacent initial tool paths on the impeller channel surface is a_e, so the *Z*-axis coordinate value of the point O_{i+1} is calculated as follows:

$$Z_{i+1} = \alpha_e \times i, i \in [1, n]$$

where n represents the number of the tool paths. Due to the initial CL point distributed on the impeller channel surface, so there must be existing local interference in the initial CL point $(X_{i+1}, Y_{i+1}, Z_{i+1})$. Hence, in order to avoid local interference, the cutter is moved along direction of the tool axis away from the impeller channel surface. Meanwhile, the method addressed in Section 2.2 is used to determine whether there is interference; if there is interference, the cutter is continued to move until there is no interference. Then, the CL point is recalculated after moving, and the CL point in the machine coordinate system without interference can be found as follows:

$$\begin{cases} X_{M_{i+1}} = X_{i+1} + T_{i+1}(x) \cdot d \\ Y_{M_{i+1}} = Y_{i+1} + T_{i+1}(y) \cdot d \\ Z_{M_{i+1}} = Z_{i+1} + T_{i+1}(z) \cdot d \end{cases} \quad (10)$$

where d is the moving distance, and T_{i+1} is the current tool orientation.

3.2 The calculation of tool orientation

Because the tool orientation can be represented by the valid angle, so the tool orientations of the whole impeller channel machining can be obtained by interpolating the valid angle of each corresponding CL point on both sides of the cleanup tool paths. So, the valid angle of each CL point on either side of the cleanup tool path is calculated first, and the calculation procedure is presented in the following steps:

Step 1 Suppose the CL point of cleanup tool path on one side of the impeller channel is $S_i(i=1,2,\ldots,n)$, where n is the number of the CL point, it is same as the number of the tool paths distributed on the impeller channel surface. The valid angle ranges of each CL point can be noted as $w_i=[\beta_{i,\min}, \beta_{i,\max}]$, $i \in [1,n]$, and the valid angle ranges of all the CL points can be represented as $\{w_1, w_2 \ldots w_i \ldots w_n\}$. Find out the maximum element in the sequence $\{\beta_{1,\min}, \beta_{2,\min} \ldots \beta_{i,\min} \ldots \beta_{n,\min}\}$ and record it as p, and then find out the minimum element in the sequence $\{\beta_{1,\max}, \beta_{2,\max} \ldots \beta_{i,\max} \ldots \beta_{n,\max}\}$ and record it as q.

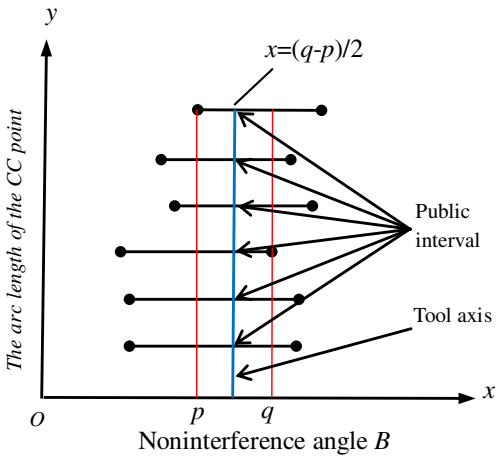

Fig. 6 Existing public interval

Step 2 If $p \le q$, it specifies that there is a public interval of the valid angle ranges that correspond to the tool orientations of every CL point $S_i(i=1,2,\ldots,n)$, so the tool orientations of all the CL points must have a same valid angle β, and $\beta=(q-p)/2$, as shown in Fig. 6, where x is the value of valid angle β, and y is the arc length between the current CL point and the initial CL point.

Step 3 If $p > q$, it specifies that there is no public interval of the valid angle ranges that correspond to the tool orientations of every CL point $S_i(i=1,2,\ldots,n)$. A rectangular coordinate system is built to obtain the valid angles of every CL point in this situation, as shown in Fig. 7, where x is the valid angle β, and y is the arc length between the current CL point and the initial CL point. There is a one-to-one correspondence between the arc length and the valid angle ranges $\{w_1, w_2, \ldots, w_n\}$ of every CL point in the coordinate system (see Fig. 7). The interval w_1 and w_n is divided into $k-1$ equal to subintervals, respectively, and the nodes of the subintervals are represented as $\{u_1, u_2, \ldots, u_k\}$

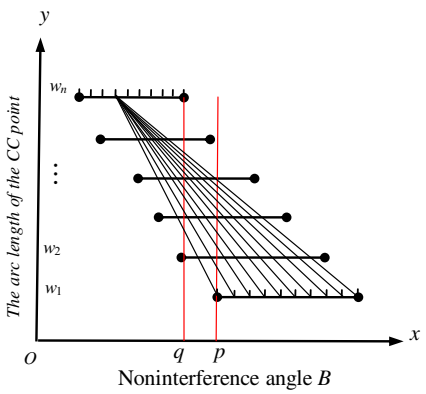

Fig. 7 No public interval

Table 1 Determine parameter of the largest cutter size

Cutting line	Intersection of valid angle (°)/radius (mm)					
	4	5	6	7	8	9
Left cleanup	(−21.19°, 3.60°)	(−21.60°, −1.33°)	(−22.79°, −6.52°)	(−23.54°, −12.02°)	(−24.21°, −17.86°)	∅
Right cleanup	(−173.78°, −163.22°)	(−169.76°, −163.24°)	(−166.43°, −163.25°)	(−163.58°, −161.81°)	∅	∅

and $\{v_1,v_2,\ldots,v_k\}$. Connect the subinterval nodes $u_i(i\in k)$ and $v_j(j\in k)$ in sequence, and then, $k\times k$ straight lines can be obtained, and the linear equation is represented as follows:

$$ax + by + c = 0$$

where a, b, and c are coefficient.

Step 4 Among the valid angle ranges $[\beta_{i,\min},\beta_{i,\max}]$ $(i=1, 2,\ldots,n)$ that correspond to the tool orientation of every CL point, the value $\beta_{i,\min},\beta_{i,\max}$ and arc length y_i of the CL point are brought to the function $g(x,y)=ax+by+c$, respectively. So the function can be expressed as

$$\begin{cases} g_1 = a\beta_{i,\min} + by_i + c \\ g_2 = a\beta_{i,\max} + by_i + c \end{cases}. \tag{11}$$

If the valid angle $[\beta_{i,\min},\beta_{i,\max}]$ $(i\in[1,n])$ of every CL point on the cleanup tool path can make the inequality equation $g_1 \times g_2 \le 0$ to be established, then the valid angle β of all the CL points can be obtained by interpolating along this straight line.

Step 5 Find out these lines which satisfy the interpolation condition and form a set G. If the set G is not void, the line of the set G with the maximum absolute value of slope is selected as the final interpolation line in order to make the change of two adjacent tool orientations minimal. Then, the valid angle β of every CL point on the cleanup tool path can be obtained by interpolating along this line. If the set G is void, the valid angle of every CL point on the cleanup tool path can be expressed as

$$\beta_i = \left(\beta_{i,\min} + \beta_{i,\max}\right)/2, i = 1, 2, \ldots, n$$

where $\beta_{i,\min}$ and $\beta_{i,\max}$ are the minimum and the maximum valid angle of a CL point S_i.

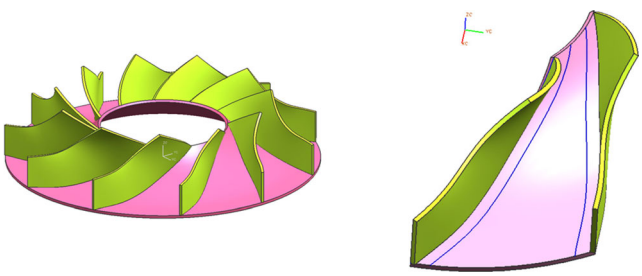

Fig. 8 Impeller model

Step 6 Use the above approach to calculate the valid angles of all the CL points on another cleanup tool path of the impeller channel. Then, interpolate the valid angle of the CL points that corresponds to each other on both cleanup tool paths, and the valid angle of the tool orientation in the impeller channel machining can be obtained after interpolation.

4 A machining simulation and verification

In order to verify the correctness and effectiveness of the proposed method in this paper, the proposed method has been realized by MATLAB programming language and implemented on machining a free-form surface impeller part. Figure 8 is the CAD model of the impeller part, the impeller with 11 blades, and the height is about 50 mm, the inner diameter is about 45.88 mm, outside diameter is about 111.5 mm, the narrowest width of impeller channel is about 24.185 mm, the blade surface is a free-form surface, and the highest height of which is about 39.35 mm.

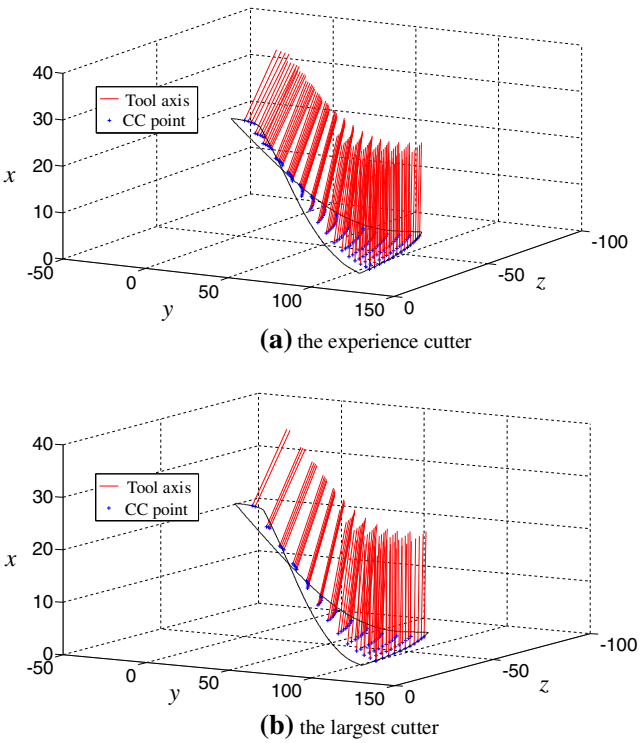

Fig. 9 Comparison of different tool paths. **a** The experience cutter. **b** The largest cutter

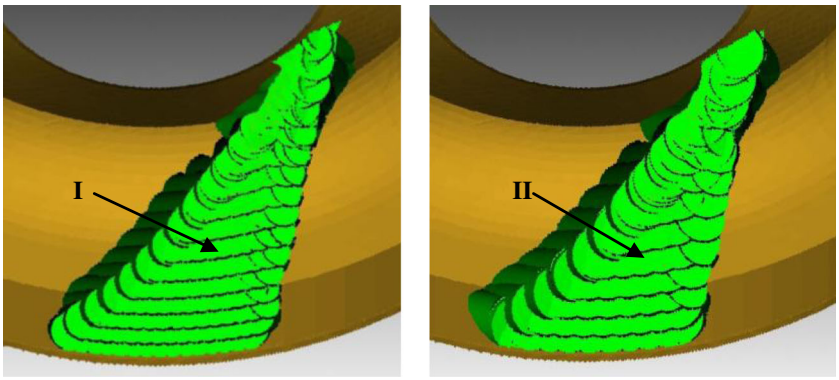

Fig. 10 Plunge milling simulation with different cutters. **a** The experience cutter. **b** The largest cutter

(a) the experience cutter **(b)** the largest cutter

Table 1 shows the largest cutter size for five-axis machining of the impeller (see Fig. 8) using the method described in Section 2. It can be seen from Table 1 that the intersection of valid angle of the left cleanup tool path is void when the cutter radius is 9 mm, but the intersection of valid angle is [−24.21°, −17.8°] when the cutter radius is 8 mm. Therefore, the largest cutter radius for the left cleanup machining is 8 mm. It can also be seen from Table 1 that the intersection of valid angle of the right cleanup tool path is void when the cutter radius is 8 mm, but the intersection of valid angle is [−163.58°, −161.81°] when the cutter radius is 7 mm. Therefore, the largest cutter radius for the right cleanup machining is 7 mm. So the largest cutter radius for machining the whole impeller is 7 mm. Compared to the experience cutter (radius=5 mm), the cutter size (radius=7 mm) is significantly increased by using the presented algorithm in this study.

After the determination of machining cutter size, the tool path of plunge milling with the largest cutter and the experience cutter are calculated using the algorithm presented in Section 3, respectively, and the tool orientation of the tool path that corresponds to the largest cutter is calculated using the presented method in Section 3 (see Fig. 9b), but the tool orientation of the tool path which corresponds to the experience cutter is obtained using the normal vector of the impeller channel surface (see Fig. 9a). Figure 9 shows two kinds of cutting tool path and the tool orientation calculated by two different machining cutters. It can be seen from Fig. 9 that the trajectory points of the largest cutter are sparser than the experience cutter, although the tool path calculation method is the same as each other.

Figure 10 shows the simulation result of the impeller plunge milling using the largest cutter and the experience cutter, respectively. It can be seen from Fig. 10 that there are no obvious pits and high residual metals in the machined surfaces I and II, and it illustrates that the tool path planning method is effective. Moreover, the tool path of the largest cutter is less than the experience cutter in the visual display of Fig. 10. In order to illustrate this issue, the NC machining tool path length L of both cutters is compared, and the result shows that the NC machining tool path using the largest cutter (L=9,315.3 mm) can be reduced by 43.9 % compare to the experience cutter (L=16,596 mm), which is consistent with the visual display of Fig. 10.

In order to further illustrate the presented method, a contrast machining test is carried out on the Cincinnati Milacron H5-800 five-axis milling center by using two cutters of different sizes for plunge milling an impeller channel, respectively. The cutters are plunger of 10 and 14 mm in diameter, and the length of cutter holder is 95 mm. In machining, the maximum spindle speed is 1,500 rpm and the feed rate is 850 MMPM.

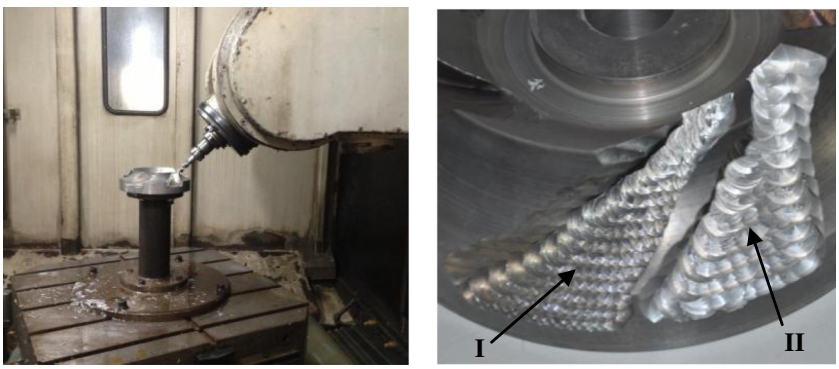

Fig. 11 The plunge milling test with different cutters in processing. **a** The machining progress. **b** The final finished results

(a) the machining progress **(b)** the final finished results

Figure 11 shows the actual machining in progress and its final shape after machining. In Fig. 11, the surface I is the final shape milled by the experience cutter, and the surface II is the final shape milled by the largest cutter. It can be seen from Fig. 11b that the actual machining tool path of the largest cutter (the finished surface II) is less than that of the experience cutter (the finished surface I) and the finished surfaces I and II of the impeller channel without pits and high residual metals. That is consistent with the simulation and calculation results (see Figs. 9 and 10). The actual machining time of the largest cutter is reduced by 28 min compared to the experience cutter, and the actual efficiency is increased by 40 %.

5 Conclusions

A new method of cutter selection and tool path generation for free-form surface impeller plunge milling is proposed in this paper. Compared with the existing plunge milling method, the main advantages of the proposed approach are as follows:

1. The cutter selection approach presented in this paper provides a theoretical basis for cutter selection for the impeller parts machining.
2. Through the establishment of constraint model between cutter size and plunge tool path, the plunge tool path can be obtained, and after actual milling, there are no obvious pits and high residual metals in the finished surface, and it verifies that the tool path plan method is effective.
3. Simulation and machining experiment shows that the plunge milling algorithm can significantly improve the efficiency of rough machining for the impeller parts.

Acknowledgments This work was sponsored by the National Basic Research Program of China (No. 2013CB035802), China Postdoctoral Science Foundation (No. 2012 M521804), and the 111 Project (No. B13044).

References

1. El-Midany TT, Elkeran A, Tawfik H (2006) Optimal CNC plunge selection and toolpoint generation for roughing sculptured surfaces cavity. J Manuf Sci Eng 128(4):1025–1029
2. Tawfik H(2009) A new algorithm to calculate the optimal inclination angle for filling of plunge-milling. Int J CAD/CAM 6(1)
3. Wakaoka S, Yamane Y, Sekiya K, Narutaki N (2002) High-speed and high-accuracy plunge cutting for vertical walls. Mate Process Technol 127(2):246–250
4. Gan WF, Fu JZ, Lin ZW, Li YC (2010) Tool-path planning based on iso-scallop for plunge milling in pocket walls manufacture. Mech Autom Control Eng (MACE) 26–28:3434–3437
5. Liang Q, Wang YZ (2011) A new rough machining approach for a ruled surface impeller. Appl Mech Mater 79(53):53–58
6. Hu CG, Zhang DH, Ren JX (2007) Research on the plunge milling of blisk tunnel. China Mech Eng 18(2):153–155, in Chinese
7. Shan CW, Zhang DH, Ren JX, Hu CG (2006) Research on the plunge milling techniques for open blisks. Mater Sci Forum: Trans Tech Publ Switzerland 532–533:193–196
8. Ren JX, Yao CF, Zhang DH, Xue YL, Liang YS (2009) Research on tool path planning method of four-axis high-efficiency slot plunge milling for open blisk. Int J Adv Manuf Technol 45(1–2):101–109
9. Nadjakova I, McMains S (2004) Finding an optimal set of cutter radii for 2D pocket machining. In: Proceedings of 2004 ASME international mechanical engineering congress and RD & D expo. IMECE 62224:2004
10. Elber G, Cohen E, Drake S (2005) MATHSM: medial axis transform toward high speed machining of pockets. Comput Aided Des 37(2): 241–250
11. Chen ZC, Zhang HD (2009) Optimal cutter size determination for 21/2-axis finish machining of NURBS profile parts. Int J Prod Res 47(22):6279–6293
12. Chen ZC, Liu G (2009) An intelligent approach to multiple cutters of maximum sizes for three-axis milling of sculptured surface parts. J Manuf Sci Eng 131:014501–014505
13. Yang ZX, Joneja A, Zhu SM (2001) Recognizing generalized pockets for optimizing machining time in process planning—part 2. Int J Prod Res 39(16):3601–3621
14. Joneja A, Yuen WF, Lee YS (2003) Greedy tool heuristic approach to rough milling of complex shaped pockets. IIE Trans 35(10):953–963
15. Yao ZY, Gupta SK, Nau DS (2001) A geometric algorithm for finding the largest milling cutter. J Manuf Process 3(1):1–16
16. Yao ZY, Gupta SK, Nau DS (2003) Algorithm for selecting cutters in multi-part milling problems. Comput Aided Des 35(9):825–839
17. Zhang YJ, Li YL (2007) New approach to selecting multiple tools for milling 2.5-D pockets. Proc IEEE Int Conf Mechtron Autom 5:2320–2325
18. Narayanaswami R, Choi Y (2001) NC machining of freeform pockets with arbitrary wall geometry using a grid-based navigation approach. Int J Adv Manuf Technol 18(10):708–716
19. D'Souza RM, Sequin C, Wright PK (2004) Automated tool sequence selection for 3-axis machining of free-form pockets. Comput Aided Des 36(7):595–605
20. Lin ZW, Shen HY, Gan WF, Fu JZ (2012) Approximate tool posture collision-free area generation for five-axis CNC finishing process using admissible area interpolation. Int J Adv Manuf Technol 62(9–12):1191–1203
21. Li LL, Zhang YF, Li HY, Geng L (2011) Generating tool-path with smooth posture change for five-axis sculptured surface machining based on cutter's accessibility map. Int J Adv Manuf Technol 53(5–8):699–709
22. Roy D (2005) Study on the configuration space based algorithmic path planning of industrial robots in an unstructured congested three-dimensional space: an approach using visibility map. J Intell Robot Syst 43(2–4):111–145
23. Sandvik Coromant (2006) "High productive milling" user's guide. http://www.sandvik.coromant.com